Effects of cation in sulfate, chloride and nitrite on $Ca(OH)_2$ activated ground granulated blast-furnace slag

Qi Zhai [a], Kiyofumi Kurumisawa [b, *]

[a] Division of Sustainable Resources Engineering, Graduate School of Engineering, Hokkaido University, Japan

[b] Division of Sustainable Resources Engineering, Faculty of Engineering, Hokkaido University, Japan

Abstract

This study explored the effects of cation in sulfate, chloride and nitrite on calcium hydroxide activated blast furnace slag. Through the use of X-ray diffraction, thermal gravity analysis and isothermal calorimetry, it was demonstrated that all the activators investigated can improve the early strength development. Compared with chloride and nitrite, it seems the type of sulfate has evident influence during the process of slag hydration. Compared with K_2SO_4 and Na_2SO_4, $MgSO_4$ has limited promotion effects on slag hydration at early age. In $MgSO_4$, the precipitation of gypsum and brucite retard the formation of hydrates for 3 hours and limit the hydration kinetics at initial stage, however, the high concentration of sulfate ions in pore solution makes a certain amount of ettringite remain, which promote the strength development. It was also found that the mechanism of pH rise in K_2SO_4 and Na_2SO_4 is due to synergistic reactions between sulfate and $Ca(OH)_2$, while low pH in MgSO4 due to low solubility of brucite inhibit the slag dissolution, the critical pH for promoting slag hydration in this study is 13.1.

Keywords: Sulfates, GGBFS, Hydration products, Ca(OH)2-activation

1. Introduction

It is known that ordinary Portland cement (OPC) blended cement containing ground granulated blast-furnace slag (GGBFS) exhibits many advantageous properties such as increased late strength, good chemical resistance and long term durability, etc.[1–5], which has become the reason why blast furnace slag cement (BFSC) is used more and more. The use of BFSC can not only exhibit the performance similar to that of OPC, but also reduce the emission of carbon dioxide by replacing some cement with slag[6–8], which is good for the environment. However, the system containing slag has the problems of lower hydration degree at early stage and insufficient early strength although the workability can be improved,

which seriously restricts the use scene of slag[9,10].

In order to improve the early strength of BFSC, chemical additives have become a common method, although this method has some problems like the amount of additives should be restricted[11]. Alkali activated BFSC system has been widely studied. Many studies show that alkali activated system can obtain the strength equivalent to that of OPC in the early stage and exceed that of OPC in the later stage of hydration[11–15]. Thomas et al. [12] reported the improvement of micro and macro properties of BFSC by sodium silicate in alkali activated BFSC system. Nguyen et al.[13] investigated the effects of sodium sulfate (Na_2SO_4), gypsum ($CaSO_4 \cdot 2H_2O$) and sodium silicate on the early characteristics of BFSC and concluded that Na_2SO_4 can shorten the setting time and enhance the early strength of BFSC. However, the phase of these systems is too complex to distinguish the respective effects of these additivities on the part of cement and slag. Therefore, many researchers have studied alkali activated slag system alone[6,15–18]. In the alkali activated slag system, the type and dose of alkali activator are important factors affecting the strength development[15,18]. Jimenez et al.[19] investigated the effects of sodium hydroxide (NaOH) and sodium carbonate (Na_2CO_3) on slag hydration, reporting that the initial pH and anion of activator plays a decisive role in the strength development of slag. Song et al.[20] showed the effects of pore solution on alkali activated slag system. When pH was higher than 11.5, the hydration reaction of slag accelerated. At present, most studies analyze the influence of anions in activators on alkali activated slag. On the one hand, in these systems, the mobility of anions is much higher than that of cations in the early stage of hydration[5,21]. On the other hand, it is difficult for cations in pore solution to have specific chemical interactions and the cations are adsorbed on the surface of hydration products by physical adsorption in order to achieve charge neutrality[22–24]. Depending on the system, there are some studies that have looked at cations in activator[21,25,26]. Edwards et al.[21] found that the effects of cations in soluble inorganic salts on the early hydration of OPC is ranked as: $Ca^{2+} > Mg^{2+} > Li^{+} > Na^{+} > H_2O \gg Zn^{2+}$. The research by Myrdal et al.[27]came up with a similar result. Sun et al.[25] studied the effects of various common cations in alite pastes mixed with simulated seawater on the micro mechanical properties, in which the deleterious effect of Mg^{2+} on the micro mechanical properties is dominant. De Weerdt et al.[28] reported the effect of various cations in chloride salts on the chlorine binding capacity of Portland cement paste. The chlorine binding capacity of Mg^{2+} and Ca^{2+} is lower than that of Na^{+} due to the effect of pH.

Sajid et al.[29] studied that the electricity charge and size of cation plays an important role in the modification of slag structure. Calcium hydroxide ($Ca(OH)_2$) activated slag is an important system to simulate the partial reaction of slag in BFSC. At present, few researchers have investigated the effect of cations of various additives on the early hydration of $Ca(OH)_2$ activated slag.

In this study, we first investigated the effects of chlorides (KCl, NaCl and $MgCl_2$), nitrites (KNO_2, $NaNO_2$ and $Ca(NO)_2$) and sulfates (K_2SO_4, Na_2SO_4 and $MgSO_4$) on the strength development, phase assemblage, hydration kinetics and degree of reaction of slag. The effects of chlorides and nitrites with different cation are similar from early to late age and there are no special hydrates formed due to the influence of different cation in the same kind of salt. However, the effects of sulfates seem quietly depend on the cation type and deserve further investigation.

At present, sulfate, especially Na_2SO_4, has been widely studied as an effective activator of slag hydration[13,16,30–33]. Na_2SO_4 mainly increase the pH value of the pore solution and promote the slag dissolution, as shown in the following formula[11,32,33]:

$$Na_2SO_4 + Ca(OH)_2 + 2H_2O \rightarrow CaSO_4.2H_2O \downarrow + 2Na^+ + 2OH^- \quad (1)$$

Our previous studies have concluded that Na_2SO_4 has a very evident effect on the early hydration of $Ca(OH)_2$ activated slag system[32]. On the one hand, Na_2SO_4 improves the pH and promotes the formation of ettringite (AFt), on the other hand, it is related to limiting equivalent ionic conductance ((LEIC) indicating the ionic mobility in solution) of sulfate ion (SO_4^{2-}), the mobility of SO_4^{2-} in the early hydration of slag is faster than other anions like NO_2^-, NO_3^- and Cl^-, which may penetrate into the hydrates and exchange with OH^- effectively[5]. However, few researchers have studied the effect of other sulfate on $Ca(OH)_2$ activated slag system. The effect of pH and sulfate on the system remains to be confirmed:

$$XSO_4 + Ca(OH)_2 + 2H_2O \rightarrow CaSO_4.2H_2O \downarrow + XOH \quad (2)$$

where X represents the corresponding cation.
Kurumisawa [34] reported that in the $Ca(OH)_2$ activated slag system, calcium sulfate ($CaSO_4$) is difficult to affect the system because the Ca^{2+} concentration is too high and the solubility of $CaSO_4$ is very low. Therefore, this study mainly investigated the effect of different cations in three kinds of sulfate (K_2SO_4, Na_2SO_4 and $MgSO_4$) on the hydration of slag to fill the above-mentioned knowledge gap.

2. Materials and methods

2.1. Materials and sample preparation

The $Ca(OH)_2$ activated slag pastes were prepared by mixing a commercial GGBFS (ST60) provided by NIPPON STEEL (Specific surface area is 4000 cm^2/g compliant with JIS A 6206) with $Ca(OH)_2$ powder (KANTO CHEMICAL CO., INC), which were the same as those used in our previous research[32]. The chemical composition of GGBFS and $Ca(OH)_2$ detected by X-ray fluorescence (XRF) is presented in Table. 1. The GGBFS is mainly made of amorphous with a broad hump between 25 and 35° 2θ, which was the analyzed by X-ray diffraction (XRD) in Fig. 1. Fig. 2 shows the particle size distribution of slag and $Ca(OH)_2$. The chosen dosage of activators was based on the previous study and except to enhance the early strength properly considering the limitation of sulfate content in slag paste[11]. Moreover, for the sake of working environment, strong alkalis present a hazard to handle[35]. Therefore, the activators were prepared by dissolving analytical-grade chlorides, nitrites and sulfates provided by KANTO CHEMICAL CO., INC (purity > 99%) in deionized water with the dosage of 0.1mol /kg and placed at ambient temperature for 1 day to ensure full dissolution.

Table 2 shows the mix proportions and undertaken tests of pastes. The pastes with 80% slag and 20% $Ca(OH)_2$ and a water/binder ratio 0.55 were prepared. For mixing, slag and

$Ca(OH)_2$ were firstly placed in the bowl of a 5-L HOBART mixer for low-speed mixing of 30s to achieve homogeneity. Then the pre-prepared activator was poured for low-speed mixing for 90s and resting for 30s, the binders on the edge and blade were scraped down by trowel. Finally, the binders were mixed at high speed for 120s. For mortar, the water/binder ratio was also 0.55. The binder/sand ratio was 1:3 and the same mixing regime was used for the mortar. The mortar was molded with cylinder (50mm diameter and length 100mm) and paste was cast into a plastic cylinder (50mm diameter and length 50mm) and vibrating for 30s to remove air. After casting, the molds were immediately covered parafilm to minimize carbonation and moisture exchange with air and placed in the special specimen curing chamber until the specific testing age of 3, 7 and 28d, which are typically used. The curing temperature was maintained at 20°C and the relative humidity was above 98%.

The mortars were used for the mechanical test, and the pastes were used for microstructural analysis. At specific testing age, the pastes were crushed into smaller particles by hammer and passed through a sieve with a size of 2-5mm. Around 1g of the particles was used for the loss of ignition (LOI). To terminate the hydration of the left particles, the solvent exchange method was used. The particles were treated with acetone and after stopping hydration, some of them were grounded into fine powder by hall mill. The powder samples were reserved in vacuum condition until the testing day for XRD, scanning electron microscope (SEM), thermogravimetric analysis (TGA) and selective dissolution.

Table 1

Chemical composition of GGBFS and $Ca(OH)_2$

	Chemical composition (wt%)										
BFS	CaO	SiO_2	Al_2O_3	MgO	SO_3	Fe_2O_3	TiO_2	Na_2O	K_2O	MnO	Others
	41.7	33.8	13.9	7.5	0.6	0.8	0.5	0.4	0.3	0.2	0.1
$Ca(OH)_2$	$Ca(OH)_2$	$CaCO_3$	Others								
	97.5	1.0	1.5								

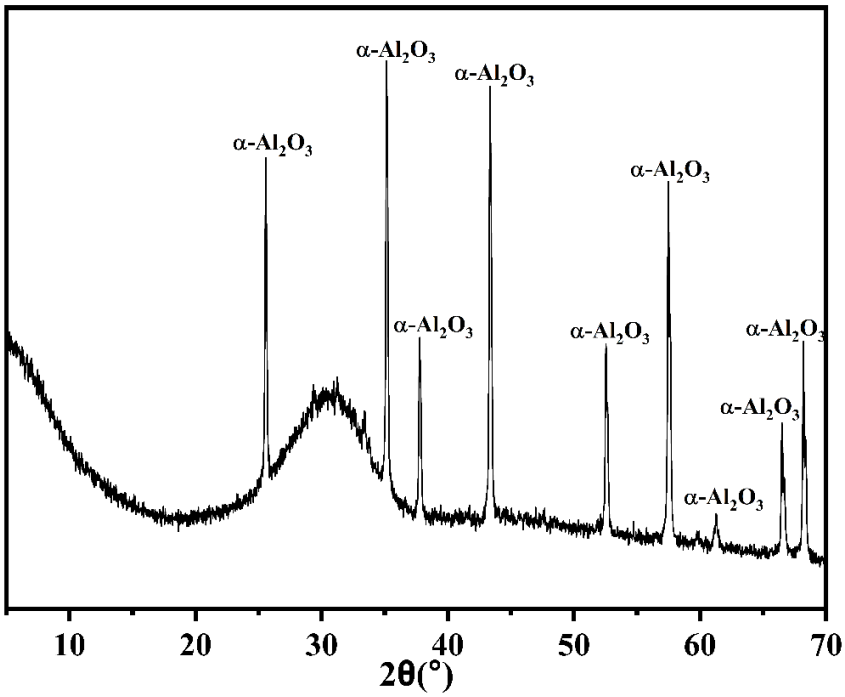

Fig. 1. X-ray diffraction of raw GGBFS

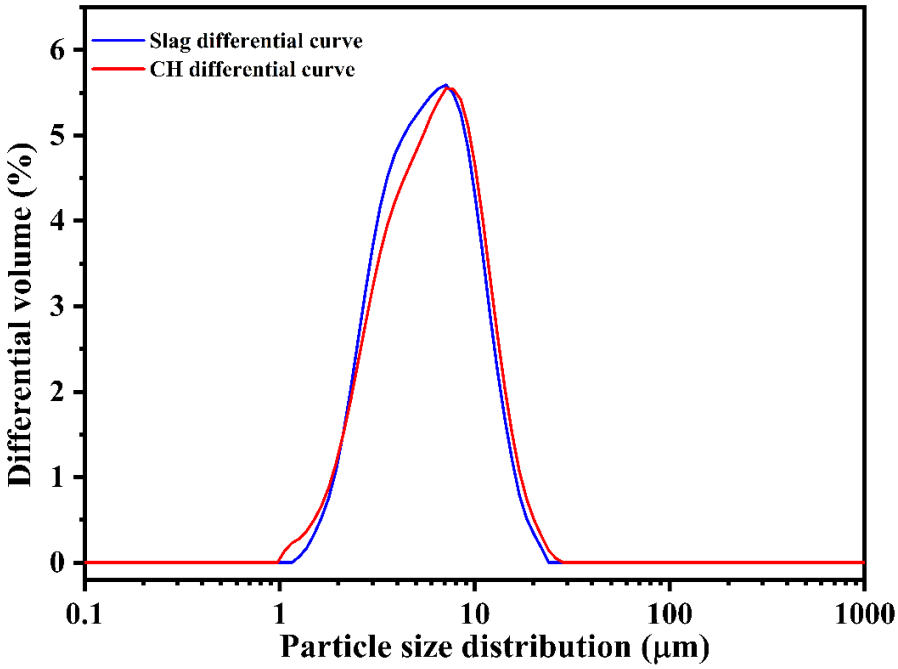

Fig.2 Particle size distribution of raw materials

Table 2

Mix proportions and tests of pastes

Mix ID	Slag (wt%)	CH (wt%)	w/b ration	Activator (wt%)	Test						
					CS	XRD	IC	SD	TGA	SEM	PSA
Con	80	20	0.55	-	×	×	×	×	×	-	×
NS				1.42%	×	×	×	×	×	-	×
KS				1.74%	×	×	×	×	×	-	×
MS				2.46%	×	×	×	×	×	×	×
KC				0.75%	×	×	×	×	-	-	-
NC				0.59%	×	×	×	×	-	-	-
CC				1.11%	×	×	×	×	-	-	-
MC				2.03%	×	×	×	×	-	-	-
KN				0.85%	×	×	×	×	-	-	-
NN				0.69%	×	×	×	×	-	-	-
CN2				1.51%	×	×	×	×	-	-	-

Note: CS-Compressive strength; IC-Isothermal calorimetry; SD-Selective dissolution; PSA-Pore solution analysis.

2.2. Compressive strength

On 3, 7 and 28d, the mortars were demolded. The compressive strength was measured on triplicate tests using an automatic testing machine (Hi-ACTIS-2000) with a constant load rate of 0.4N/mm^2·Sec. An average value with standard derivation was reported as the compressive strength.

2.3. X-ray diffraction

Powder X-ray diffraction analysis for the powder samples was performed by an X-ray diffractometry (XRD, Multiflex, Rigaku Co., Ltd., Tokyo, Japan) with Cu-Kα radiation under 40 kV voltage and 40mA current. The powder was scanned at the range of 5-70° (2θ) at a step size of 0.02°/min and scanning speed of 2°/min to investigate the crystalline phases. 20% α-Al_2O_3 was added as internal standard to quantify the amorphous phase. The quantification of hydrates was investigated using Profex[36].

2.4. Isothermal calorimetry

The hydration heat of $Ca(OH)_2$ activated slag mixed with activator was evaluated using a isothermal calorimeter (MMC-5116; Tokyo Riko). Before testing, the internal temperature of the chamber was set at 20°C and kept for 1d to maintain stability. Internal automatic mixing method cannot guarantee homogeneity and sufficiency, therefore external manual mixing method is adopted[37]. Before mixing, the pre-prepared activators were placed at 20°C for 1 night to ensure full dissolve and reduce the error caused by internal and external temperature difference. The binder above 20g was mixed externally for 5min in 100 ml ampoule, and the binder was placed in the calorimeter quickly. Because the temperature difference inside and outside the chamber is unavoidable, the initial 1 hours' measurement was omitted.

2.5. Selective dissolution

The reaction degree of slag was determined by selective dissolution based on EDTA. EDTA solution was prepared with 250 mL triethanolamine (TEA), 93g Ethylenediaminetetraacetic acid (EDTA) dissolved in 500 mL distilled water and 173 mL diethylamine (DEA) and dilute the solution to 1L[38]. The dissolution test was performed with 0.5g±0.02g powder. Before test, the powder and cellulose acetate filter papers with 4.5 μm pore size (Toyo Roshi Kaisha, Ltd) were dried in a 105°C oven for 1h to avoid moisture exchange. Before the test, the dissolution of raw slag was measured to determine the undissolved proportion of the material, around 5±1 wt% slag dissolved, which was below 10 wt% [38]. The powder was mixed with 50 mL EDTA solution in a beaker, then dilute to 800 mL with distilled water, which was stirred at 300 ppm for 2h with a magnetic stirrer continuously. The residue was dried in a 105°C oven for 1h until the weight was stable. Then, the weight of the residue was calculated. After weighing, the residue was gathered for XRD test. The hydrotalcite-like phase, as a kind of main phase generated during the hydration of slag, cannot be dissolved by EDTA solution, therefore in this study, the assumption was made as follows: all the MgO was converted into hydrotalcite like phase, so that the mass of hydrotalcite-like phase can be calculated at a mass ratio of 1:2.35[39]. The reaction degree (α) of slag was calculated based on the formula as follows:

$$\alpha = \frac{100fR_s - R_r}{100fR_s - 2.35fM_{MgO}} \quad (3)$$

where f is the mass fraction of GGBFS in dry binder, R_s is the mass fraction of GGBFS undissolved in EDTA solution, R_r is the mass fraction of the residue in g/100g anhydrous binder, M_{MgO} is the mass of MgO in GGBFS.

Since the powder used in the dissolution test is from dried composite particles, 100g dried composite pastes are converted to anhydrous binder using the following formula[38]:

$$m_{anhydrous} = \frac{m_{dried\ composite\ paste}}{1 - LOI} \quad (4)$$

where $m_{anhydrous}$ is the mass of anhydrous binder, $m_{dried\ composite\ paste}$ is the mass of dried composite paste and LOI is the nonevaporable water content of the dried composite paste.

To determine the LOI of the binder, around 1g of the particles was dried in a 105°C oven for 1d to obtain a relative constant mass. Then the dried particles were heated from ambient temperature to 700°C for 2h in a furnace to obtain the LOI as above 700°C, S^{2-} will be oxidized to sulfate to increase the mass[40]. The calculation formula is as follows:

$$LOI = \frac{m_{105°C} - m_{700°C}}{m_{700°C}} \quad (5)$$

where $m_{105°C}$ is the mass of particles after 105°C, $m_{700°C}$ is the mass of particles after 700°C.

2.6. TGA

For TGA, the analysis was carried out by HITACHI TG7000. About 10 mg of the powdered sample was loaded into a Platinum crucible. The powder was heated from 20 to 100 °C at a rate of 10 °C/min, under a N_2 flux of 30 mL/min. The portlandite content was measured using the tangent method.

2.7. pH of pore solution

The pH value of pore solution was measured using a pH electrode calibrated using buffer solution before the hardening of the paste. The pastes were mixed manually at 30 minutes intervals to avoid the influence of bleeding phenomenon. The pore solution was extracted by KUBOTA 3700 centrifugation (set as 4000rpm and 60s) and the gathered solutions were used for pH measurement. Once the measurement finishing, the solution was filtered with a 4.5μm filter and 5ml injection as soon as possible. After filtering, the solution was stored in a refrigerator to avoid precipitation.

2.8. Pore solution composition

To investigate the influence of sulfate salts on the early stage of hydration, the filtered pore solutions at 1, 3, 6, 9, 12, 15, 18 and 24hours were diluted by a factor of 50 for Con and 500 for other samples with distilled water. The measurement was carried out using an ion chromatography (ICS-90, DIONEX, Sunnyvale, CA, USA) to determine the concentration of SO_4^{2-} and Ca^{2+} with the cica-reagent cation mixed standard solution.

2.9. Thermodynamic modelling

Thermodynamic modelling was carried out with Gibbs free energy minimization software GEMS with CEMDATA 18 and PSI/Nagra database and CNASH model[41]. The effects of sulfate salts on the phase transformation of slag were simulated in this program based on the hydration degree calculated by selective dissolution.

2.10. SEM-EDS

SEM was used for observing the morphology of the hydration products in MS. For the specimen preparation, the powder was immersed in ethanol and treated with ultrasonic dispersion for 5 min, one milliliter of the suspension was transferred on carbon disks.

The investigation was performed with a JEOL JSM-IT200 scanning electron microscope combined with an energy dispersive spectrometer (EDS) operated at an accelerating voltage of 15 kV.

3. Results and discussion

3.1. Compressive strength

As an essential part of additives evolution, the influence of different inorganic salts on the compressive strength of the mortars were investigated, the result is shown in Fig. 3. As shown in Fig. 3(a), all of the chloride used in this study could improve the early strength of the mortar. However, from 7d, the improvement is not so evident and even lower than that of the control group and one phenomenon can be observed that although the cation in chloride

is different, the efficiency is almost same, which seems the influence of action in chloride is small. The strength development of samples added with nitrites shows the similar tendency as shown in Fig. 3(b)

It can be seen in Fig. 3(c) that in comparison with control group, KS, NS and MS increase the 1d and 3d compressive strength. At 28d, Con has the highest compressive strength. Moreover, it's noteworthy that at early strength development, KS always has the most evident promotion on the compressive strength and NS has the similar impacts, while the compressive strength of MS does not change much at 1d, at 28d, MS has higher strength than that of KS and NS and close to that of the control group.

It has been reported that sulfates could promote the development of early strength of slag [42–50] and some of the research reported that this high early promotion effect also result in the rate of late strength development reduced because of late porosity increased result from crossover effect[49], thick layer of hydrates surrounded the undissolved slag[48] and relative relationship between capillary pores and limit radius[45,46,50]. etc. The results of this study indicate that although sulfate salt promoted early strength development of mortars and reduced the development rate of late strength which is similar to the results of the researchers mentioned above, the effect of sulfate with different cation is a little different, which will be further discussed in next sections.

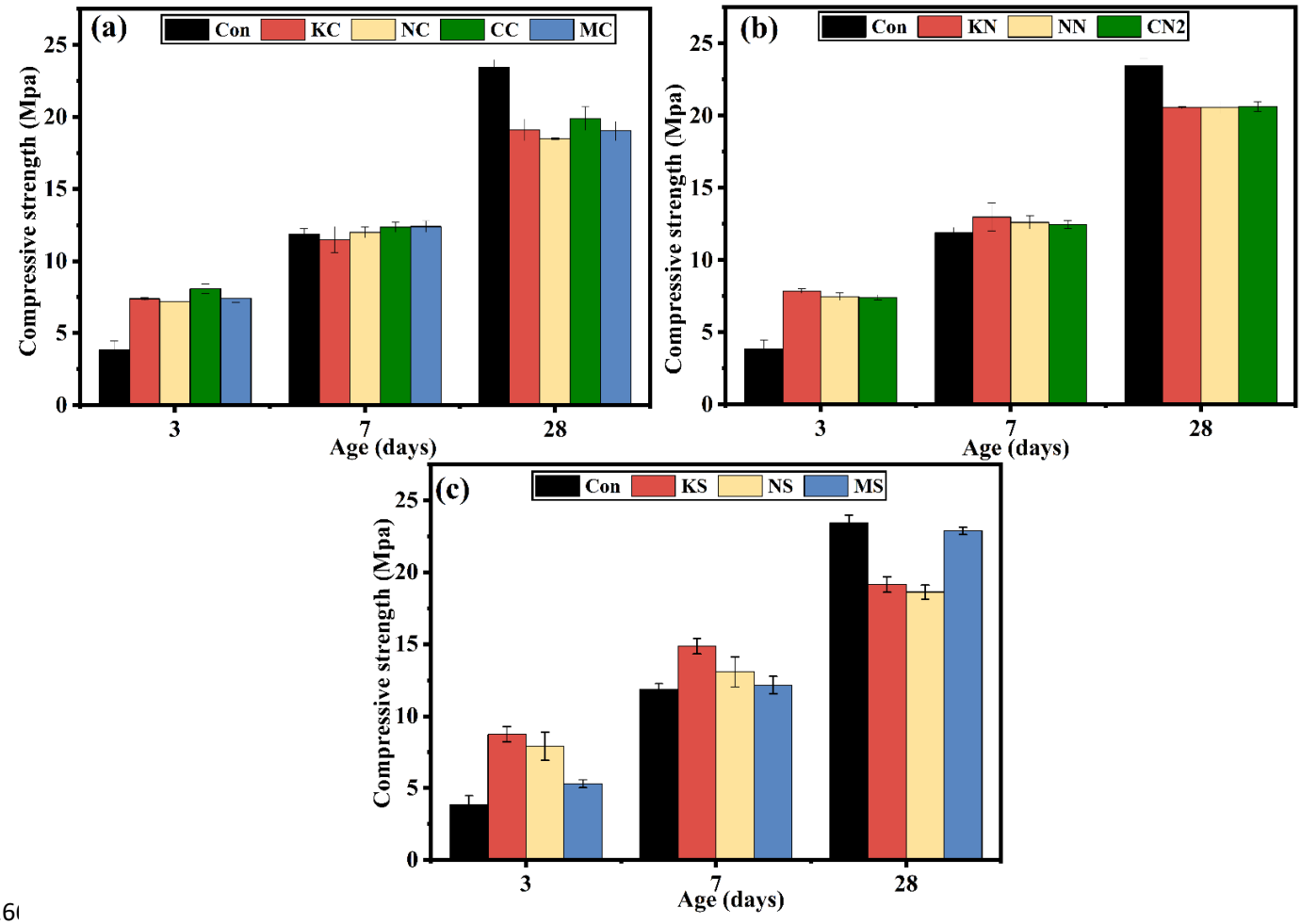

Fig. 3. Effects of different salts on the compressive strength of mortars (a) chlorides (b) nitrites and (c) sulfates,

3.2. X-ray diffraction

Fig. 4 show the XRD spectra from 5 to 35° (2θ) of samples cured at 3 and 28d. The result of samples cured at 7d are shown in supplementary data (Fig. S1).

Fig. 4(a) and Fig. 4(b) shows the XRD pattern of samples added with chloride. Instead of SO_4-AFm and AFt, Friedel's salts around 11.16°(2θ)[22,23,28] was observed. Fig. 4(c) and (d) shows the XRD spectra of samples added with nitrite. NO_2-AFm was detected at 11.08°(2θ) in each spectrum[57,58].

Fig. 4(e) illustrate the development of the hydration phase assemblage at early stage in sulfate. At 3d, ettringite (AFt), hemicarboaluminate, monocarboaluminate and hydrotalcite were identified as the main crystalline hydrates[4,51–54]. In KS, NS and MS, higher sulfate content led to the initial AFt formation increased. Compared with KS and NS, MS has much more AFt around 9°(2θ)[53] and almost no SO_4-AFm was detected, for KS and NS, not only AFt but also a certain amount of SO_4-AFm around 9.9°(2θ)[55] also formed, which is clear

shown in Fig. 7, this indicates that based on the concentration of sulfate of the same equivalent, KS and NS promoted the dissolution of slag greatly, while in MS, the relative Al^{3+} concentration was lower than that of SO_4^{2-}, although the concentration of $SO4^{2-}$ is little low, no SO_4-AFm can form. This may be the reason why the strength of MS is a little bit higher than that of control group but relative lower than that of KS and NS at 3d. In control group, ettringite content was quite small because of the absence of additional sulfate and almost no AFm-like phase was detected, instead, hemicarboaluminate formed, which may relate to the quite slow dissolution rate of slag and result in the low strength at early stage.

At 28d (Fig. 4. (f)), the same products are formed, hemicarboaluminate, AFt and monocarboaluminate as main calcium aluminate hydration products, hydrotalcite as Mg-Al layered double hydroxide. Small differences were observed. For KS and NS, the intensity of the peak of AFt is quite low compared with that of MS. For control group, the solid solution SO_4-AFm, OH-SO_4 (mainly C_4AH_{13}) around 11.30°(2θ)[56] was observed.

Although the type of hydrate changed with the change of the anion of activators, the cation of the activators seems did not change the phase transformation. Combined with the results of compressive strength, it seems cation in nitrite and chloride has little influence on the hydration development of slag. However, the sulfate is unique enough and it is necessary to understand the effects of cation in sulfate on the slag paste.

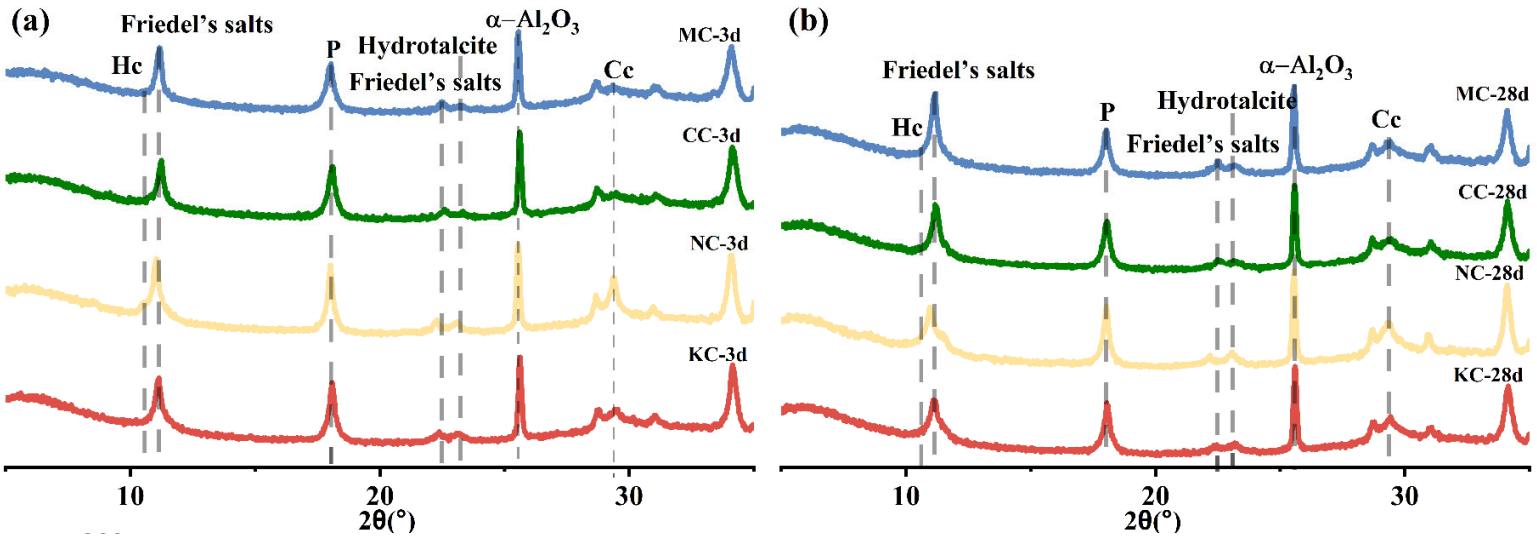

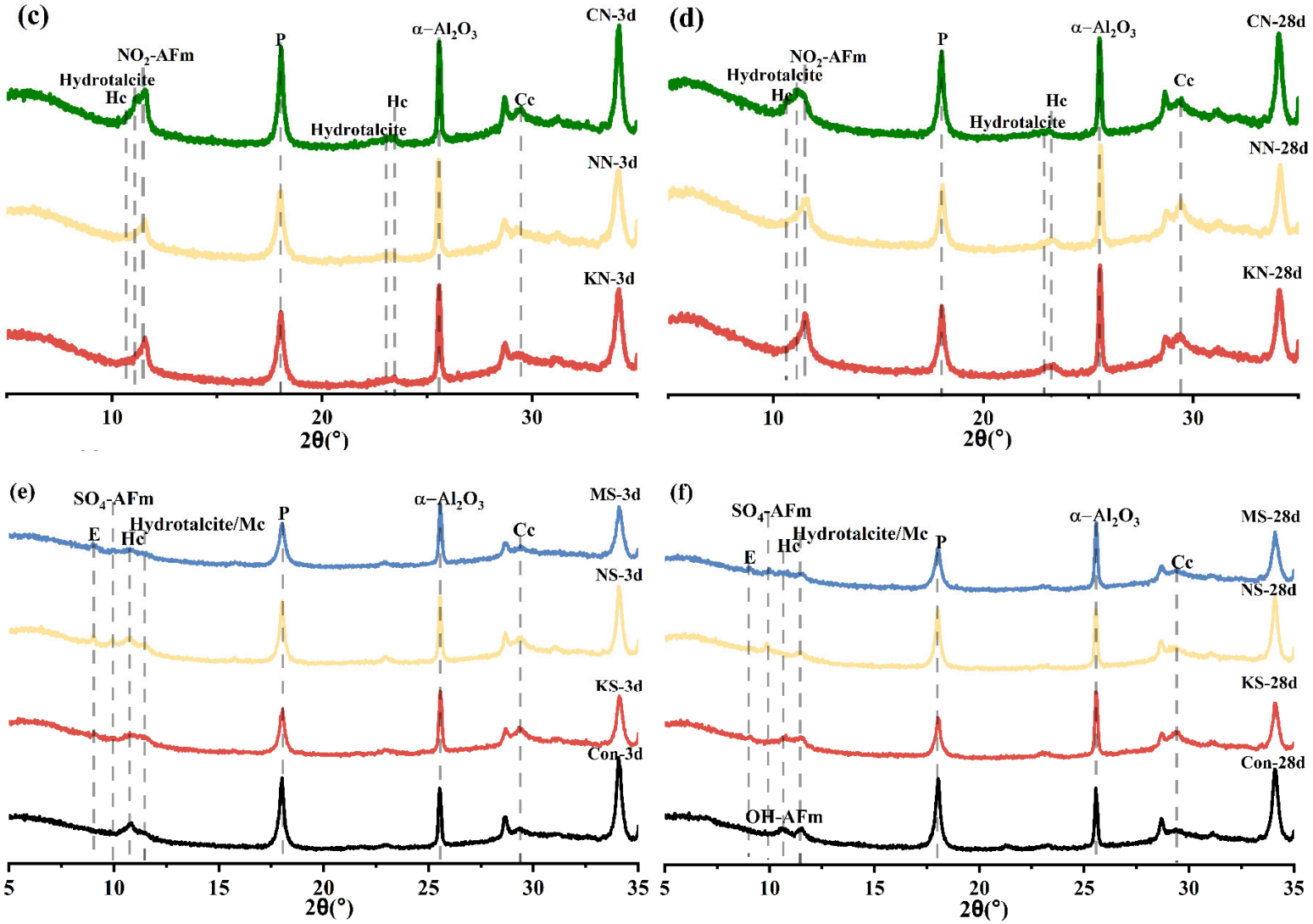

Fig. 4. XRD patterns of pastes (a) chloride curing at 3d, (b) chloride curing at 28d, (c) nitrite curing at 3d and (d) nitrite curing at 28d, (e) sulfate curing at 3d, and (f)sulfate curing at 28d. The reflection peaks are marked as follows: E stands for Ettringite, SO_4-AFm stands for calcium monosulfaluminate, Hc for Hemicarboaluminate, Mc for Monocarboaluminate, OH-AFm for hydroxy-AFm, P for portlandite and Cc for calcite.

3.3. Isothermal calorimetry

The heat flow curves and cumulative heat results of the pastes, which provide important information regarding the additives influence on hydration kinetics of pastes are displayed in Fig. 5.

Fig. 5(a) and (c) shows the hydration heat flow of chloride and nitrite, evidently all the main peak of pastes occurs later than that of control group, although all of them are higher and broader. Compared with sulfate, it seems the shape of the peak did not change in nitrite and chloride. Although CC and MC seem retard the kinetic compare with other chloride, and CN2 seem retard the hydration kinetic compared with KN and NN, the difference in cumulative heat is limit as shown in Fig. 5(b) and (d). This result is consistent with the strength development at early stage.

Fig. 5(e) represents the hydration heat flow of pastes combined with different sulfates. The main peak of Con around 9.8h, NS around 9.3h, KS around 9.85h and MS around 12.9h was attributed to the precipitation of C-(A)-S-H and ettringite, which was confirmed by XRD (Fig. S2) NS showed an almost 4 times higher and 0.5h earlier exothermic peak than that of control group around 9.3h, while KS had the similar effects. This may attribute to the activators accelerated the dissolution of slag and the additional sulfate promoted the formation of ettringite. However, for MS, it is clearly shown that the main peak of MS occurred 3h later than that of control group and the rate of the heat generation before and after 11.5h is quite different. Usually, this kind of peak presents undersulfated situation[30]. From the result of XRD (Fig.S2), a certain amount of gypsum and a small amount of brucite precipitated. This indicates that in MS, the initial kinetic was limited, which may relate to the initial lower pH value than that of other samples (Fig. 9a). Although the initial hydration of MS is slower than that of other samples, a large amount of ettringite around 5% still can be observed after 15h, which may promote the compressive strength at early age. Fig. 5(f) presents the cumulative heat of pastes, evidently the additional of KS and NS increase the overall hydration, for MS, before 12h, the cumulative heat of MS was almost same as control group, after that, the cumulative heat of MS was a little bit higher than that of control group. However, compared with KS and NS, the accumulated heat of MS was about 39% less at 3d. which is consistent with the strength development.

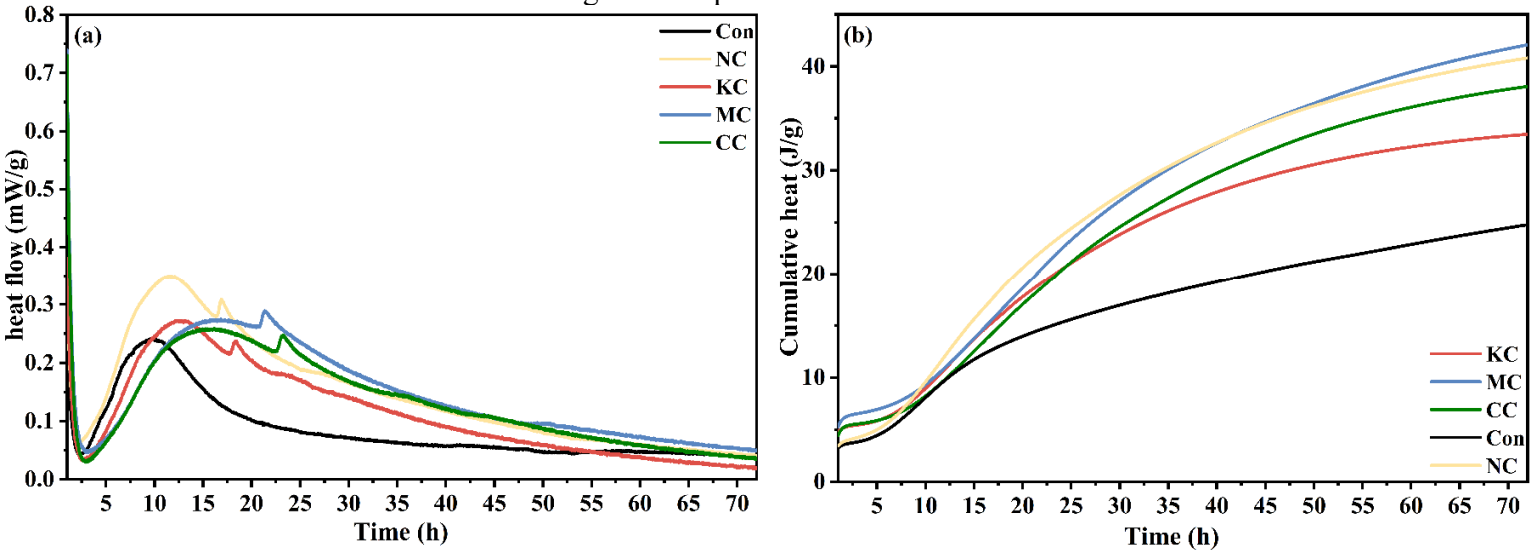

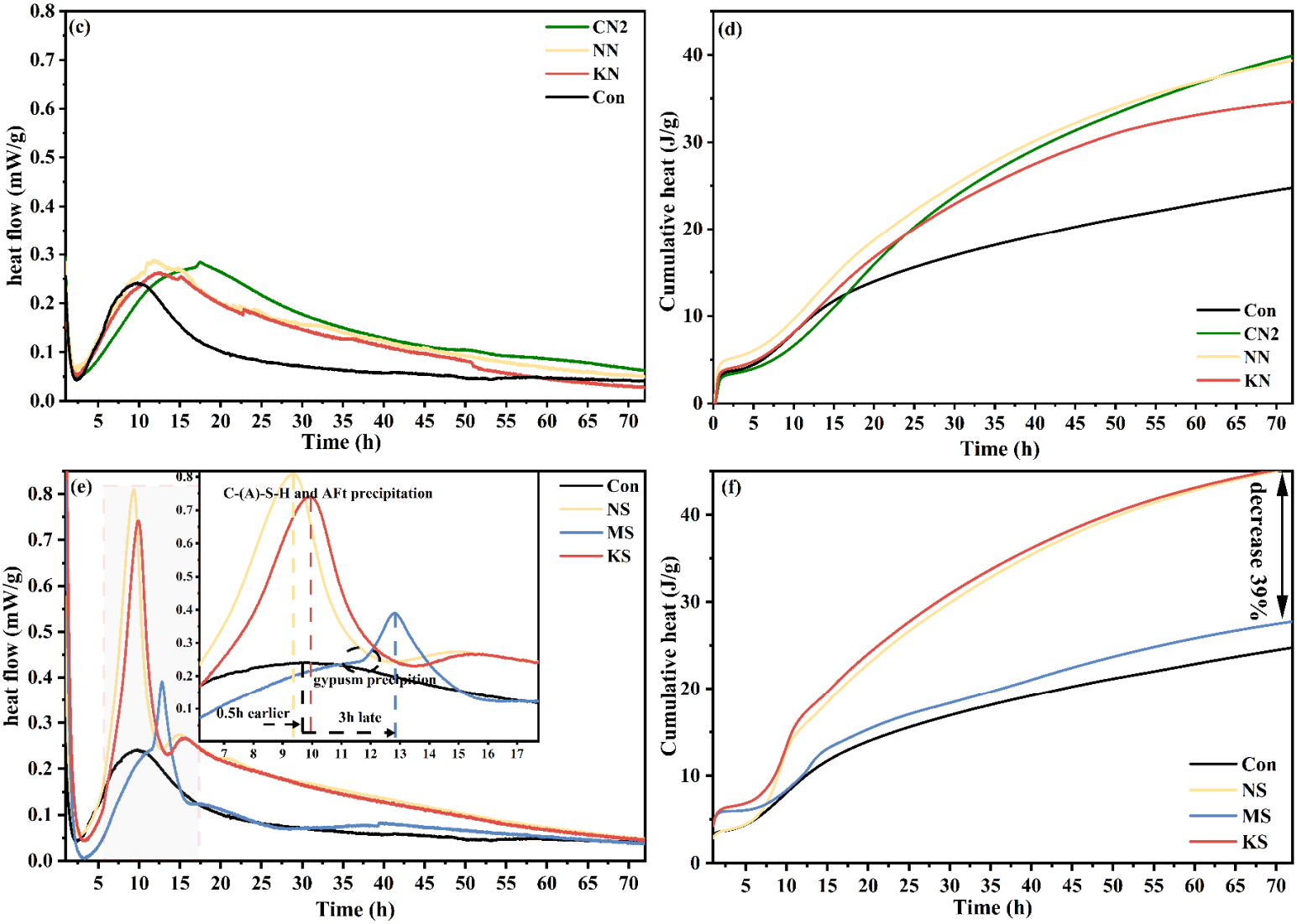

Fig. 5. Effects of chemical activators on hydration kinetics of pastes (a) heat flow of chloride, (b) cumulative heat of chloride, (c) heat flow of nitrite, (d) cumulative heat of nitrite, (e) heat flow of sulfate and (f) cumulative heat of sulfate.

3.4. Selective dissolution

Fig. S3 presents the XRD pattern of samples after selective dissolution. Evidently, after selective dissolution, only hydrotalcite and amorphous phase remained, which illustrate that the selective dissolution method is responsible in this study to some extent. The reaction degree of slag is shown in Fig. 6(a), (b) and (c). It can be seen that the overall reaction degree of samples added with activators is higher than that of control group at early age due to the high activity, which is consistent with the results of compressive strength. With further

hydration, the reaction rate of the samples added with activators increase slowly except MS, at 28d, the reaction degree of control even overpasses some samples added with activators. One interesting phenomenon is that in nitrite, although the reaction degree is different, the development rate of reaction degree is quite similar. The reaction degree difference in nitrite and chloride is slight, while in sulfate the tendency of reaction degree is quite different at early although at the late age it seems to be unified.

The relationship between reaction degree and compressive strength is shown in Fig. 6(d). The compressive strength of the samples developed quickly when the reaction degree of slag reaches more than 25%. At early age, the reaction degree quite affects the development of strength. At late stage, nonlinear correction between reaction degree and strength was observed, which indicates that some other factors influence the strength at late age, this has been discussed in the previous work[32].

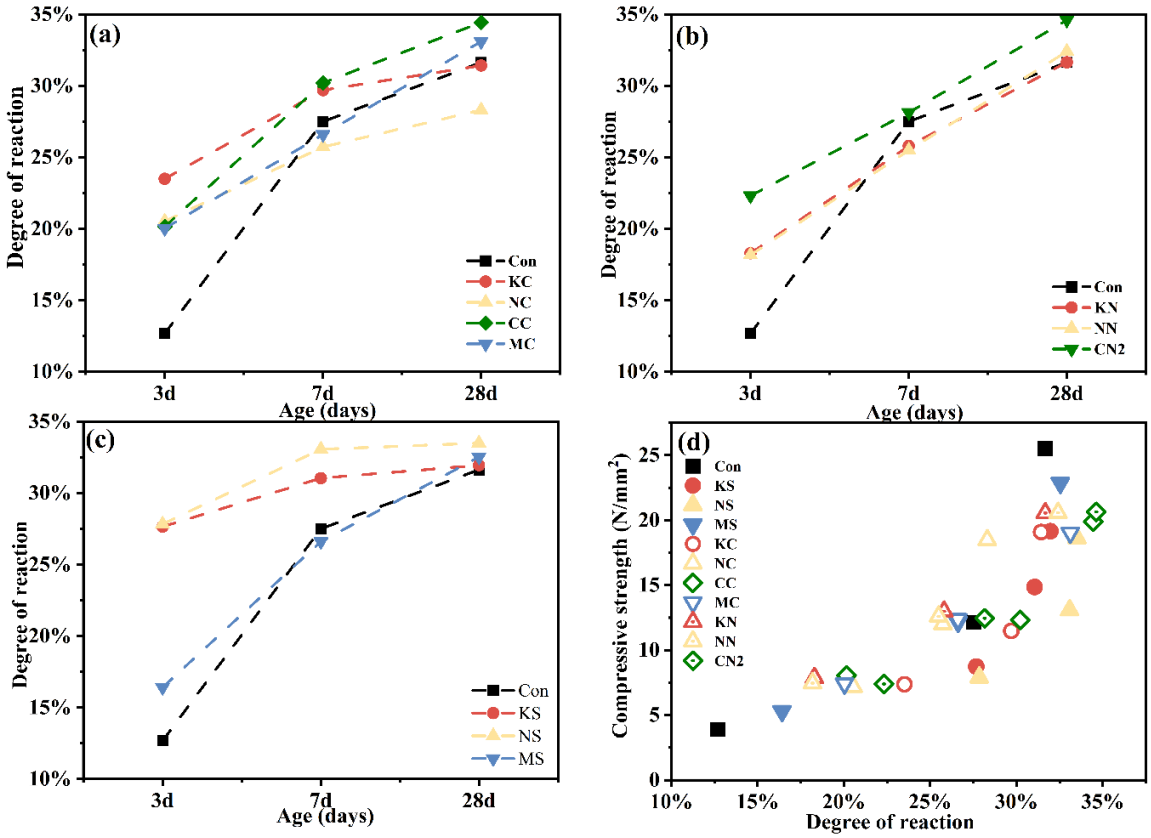

Fig. 6. (a) Reaction degree of chloride (b)Reaction degree of nitrite (c) Reaction degree of sulfate and (d) Relationship between reaction degree and compressive strength.

3.5. The effects of cation in sulfate on $Ca(OH)_2$ activated GGBFS

As discussed from section 3.1 to 3.4, although some slight difference exists in the development of hydration kinetics and degree of reaction in nitrite and chloride, the influence

of this difference is limit in the strength development and phase transformation. The phase transformation and the shape of the exothermic peak in calorimetry seems mainly influenced by the type of anion in activators. However, the kinetic rate may mainly be affected by the anion in activators, and the difference in sulfate is larger than that of nitrite and chloride even influence the shape of the exothermic peak to some extent. Therefore, combined with the result of compressive strength, the effects of sulfates seem quietly depend on the cation type, from this section, the effects of sulfate are mainly discussed.

3.5.1.QXRD

Quantification of the hydration products in sulfate by XRD is presented in Fig. 7. The content of C-(A)-S-H was determined by subtracting the amorphous phase from unreacted slag calculated by selective dissolution in section 3.4. From Fig. 7(d), it is shown that quality small amount of brucite formed not only in 3d but also at 28d. For MS, it is special because the solubility of brucite is quite low. Bernard et al.[59] investigated that at early age, the brucite precipitated and intermixed with C-S-H, with the hydration progressed, the brucite dissolved and M-S-H formed. Sun et al.[25] found that the at early age, the strength will increase because brucite decrease the porosity. However, dissolution of brucite increased the porosity and this phenomenon will decrease the hardness and modulus of pastes for long term. In this study, the phenomenon is in adverse, the initial strength development was inhibited, at 28d, the strength is a little bit higher than that of KS and NS and through this process a little brucite not above 2% was observed from XRD, which may relate to the low concentration of Mg^{2+} added in this study. Therefore, it is important to investigate the hydrates transformation of MS before 1d, which is discussed in section3.5.3. The QXRD also show the consumption of $Ca(OH)_2$, with the hydration, the amount of $Ca(OH)_2$ decreased, however, because the different additives were added, the solubility of portlandite also changed. Therefore, the consumption ratio of portlandite cannot be compared directly. The portlandite content following the same trend as TGA results.

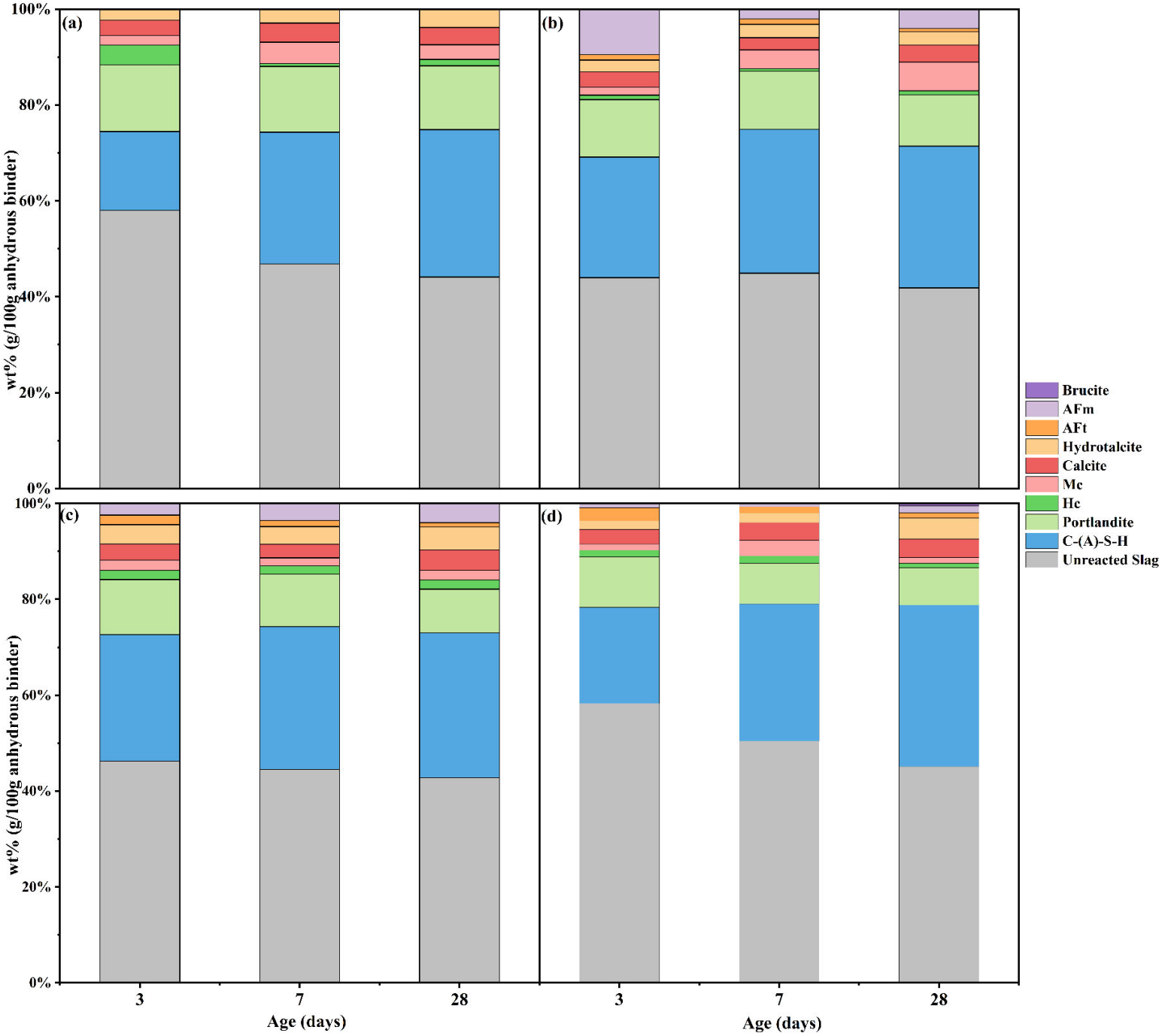

399 Fig. 7. XRD quantification results showing the major hydrates at 3, 7 and 28d of pastes (a)
400 Con, (b) KS, (c) NS and (d) MS.

401

402 3.5.2.TGA

Fig. 8 displays the TGA/DTG data of pastes cured at 3d (7 and 28d in Fig. S4), which shows the effects of additive activators on the hydration products. From the DTG curves, three peaks were clearly observed. The first peak from 80 to 200°C are considered as the weight loss of several hydrates like C-(A)-S-H, ettringite, AFm phase and hydrotalcite is in agreement with XRD analysis[60,61]. The peak between 380 to 460°C corresponding to the dihydroxylation of portlandite [60,62] was always observed from 3 to 28d in all samples. The third peak appears around 680°C, which occurs a little lower than the peak where calcite is usually located, may be related to the formation of monocarbonates and hemicarbonate or poorly crystalline carbonates due to carbonation of samples, which is consistent with the report by Durdzinski at el.[63] Compared to the control group, all of other samples show the great mass loss between 80 and 200°C, which indicates that sulfate salts greatly promote the hydration of slag. Due to the presence of C-(A)-S-H in the portlandite region, the tangential method was used to quantify the weight of portlandite[37,64]. The weight measured by TGA presents the portlandite left in the hydrate binders, the mass fraction of portlandite in anhydrous can be calculated by the formula as follows:

$$m_c = \frac{m_R}{0.243(1 - LOI)} \quad (6)$$

where m_c presents the residual mass fraction of $Ca(OH)_2$ in g/100g anhydrous, m_R presents the residual mass fraction of portlandite in g/100 binders.

The results are shown in Table.3. It should be noted that the solubility of has been changed due to the addition of activators. Therefore, the results cannot be compared directly. However, from Table. 3, it is clearly shown that the residual mass of portlandite in most of samples show volatility and large quantity of portlandite precipitate during the whole hydration process as observed. This demonstrates that although $Ca(OH)_2$ was consumed with the hydration, the solubility of portlandite changed with the activity of slag. This maybe an important factor influences the reaction degree of slag.

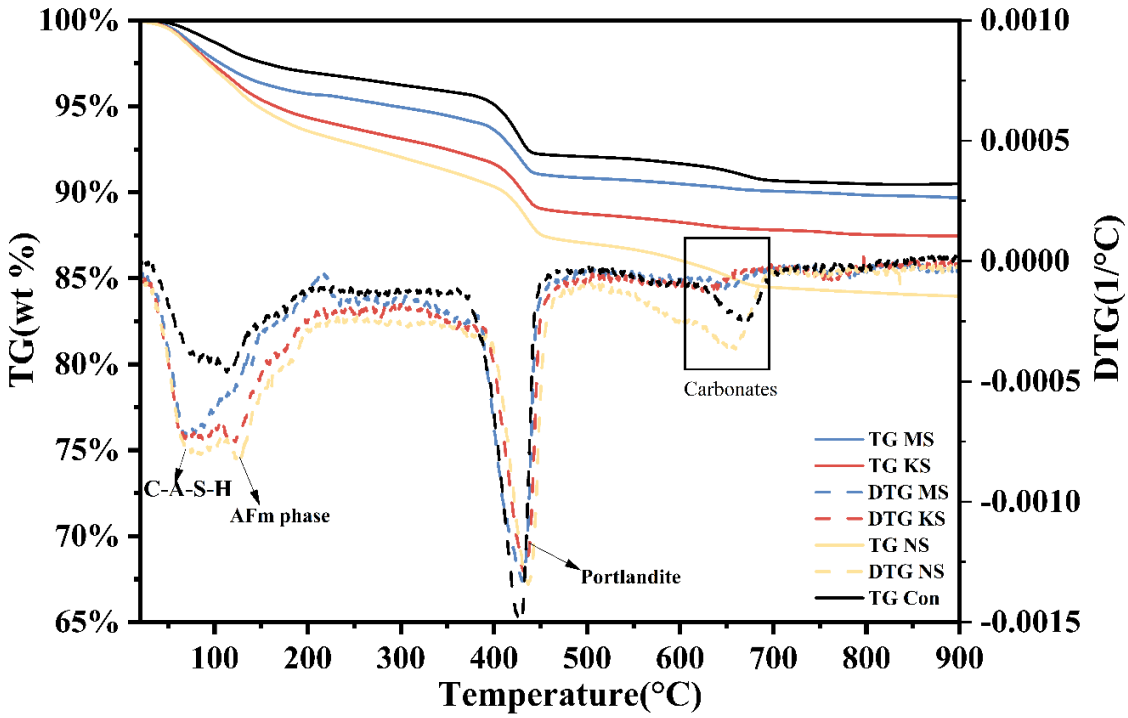

Fig. 8. TGA and DTG curves of pastes cured at 3d.

Table 3
Residual portlandite in anhydrous.

Sample ID	3d	7d	28d
Con	8.72%	12.96%	11.81%
KS	11%	9.63%	8.97%
NS	12.51%	12.09%	11%
MS	10.70%	9.96%	11.36%

3.5.3.pore solution

As discussed in section 3.3, it was found that differs from KS and NS, although MS promote the strength development at 3d, the initial kinetic was inhibited in MS. To further identify the influence of cations in sulfate at early stage, it is necessary to investigate the phase transformation and early hydration progression. The pH value of the pore solution before 1d is shown in Fig. 9(a). Evidently, KS and NS has higher pH value than that of Con and MS in the whole hydration process before 1d. For MS, it is always similar to the control group, even a little bit lower, although it is above the pH value that can promote the dissolution of slag[20]. Fig 9 (b) and (c) shows the concentration of Ca^{2+} and SO_4^{2-} in pore solution changes with time. The tendency of ion concentration in all samples is similar, a large drop was found around 12h corresponding to the large quantities of hydrations

formation, which is consistent with the result of isothermal calorimetry. Compared to KS and NS, MS and Con always has a higher ion concentration because of the low reaction rate of slag. Fig. 9(d) indicates the relationship between pH and the ion concentration. Suraneni et al.[65] reported that when the concentration of Ca^{2+} in solution is at 20 mM, it has a strong inhibiting effect on the slag dissolution, while in this study the similar phenomenon was also observed that most of the Ca^{2+} concentration in NS and KS is lower than 20 mM after 3h and this may related to high pH value (above 13.1) promoted the dissolution of slag and the hydrates consumed large amount of Ca^{2+} in the solution.

The following mechanisms explaining the changes in the pH for the pore solution in different sulfates:

For Na_2SO_4 an increase in the pH is observed, which may relate to synergistic reaction described in Eq. (1). The reaction between $Ca(OH)_2$ and Na_2SO_4 increases the concentration of SO_4^{2-} and results in the formation of more ettringite, while enough Na^+ remain in the pore solution, which need OH^- to ensure charge neutrality. The increased pH of the solution accelerates the dissolution of slag.

For K_2SO_4 the reason for increasing the pH value of pore solution is almost same as Na_2SO_4, which benefits from the fact that cations can hardly react chemically. The Eq. (7) summarized the mechanisms of pH changes in KS and NS[35]:

$$(Na,K)_2SO_4 + Ca(OH)_2 + 2H_2O \rightarrow CaSO_4.2H_2O \downarrow +2(Na,K)^+ + 2OH^- \quad (7)$$

In the case of $MgSO_4$, the $MgSO_4$ will react with $Ca(OH)_2$ and precipitate as brucite shown in Eq.(8) because of the low solubility (Fig.S2), which hence reduce the pH value and the precipitation of brucite will be attached on the surface of slag to extend the induction period (Fig. 6a) and decrease the dissolution rate of slag[66]. Moreover, high concentration of Ca^{2+} in the pore solution also inhibits the dissolution of gypsum due to the common ion effect. Such lower pH value and higher concentration of Ca^{2+} than KS and NS inhibit the reaction of slag before the paste lose its plasticity. However, as the pH value still >12.5, the slag will be dissolved slowly and Al^{3+} increase in solution consumes the gypsum (Eq.9, 10 and 11)[35,67] and increase the pH value. The formation of brucite in addition of MgO in pure water shows a pH value of 10.5, therefore, the high pH value will cause the metastable brucite dissolve slowly[59].

$$MgSO_4 + Ca(OH)_2 + 2H_2O \rightarrow CaSO_4.2H_2O \downarrow +2Mg(OH)_2 \downarrow \quad (8)$$

$$\equiv Si - O - Al \equiv +7OH^- \rightarrow [SiO(OH)_3]^- + [Al(OH)_4]^- \quad (9)$$

$$[Al(OH)_4]^- + 4Ca^{2+} + 6H_2O + 6OH^- \rightarrow C_4AH_{13} \quad (10)$$

$$C_4AH_{13} + 3CaSO_4.2H_2O + 14H_2O \rightarrow C_3A \cdot 3CaSO_4 \cdot 32H_2O \quad (11)$$

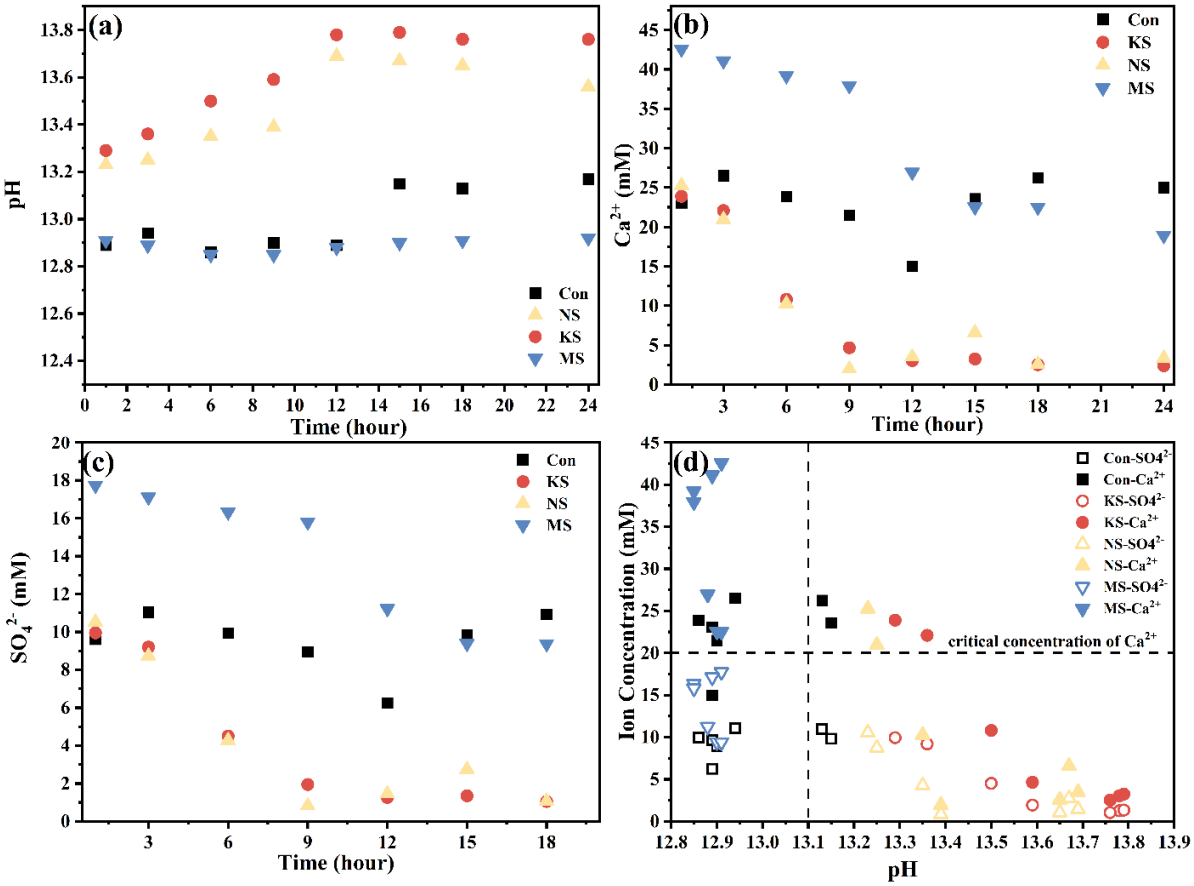

Fig. 9 pore solution of concentration and pH (a) pH, (b) Ca^{2+}, (c) SO_4^{2-} and (d) relationship between concentration of Ca^2 and SO_4^{2-} and pH.

Thermodynamic modelling was used to simulate the phase transformation of MS at low reaction degree. The reaction degree of slag before 1d was calculated based on the result of cumulative heat release:

$$\alpha(t) = \frac{Q(t)}{Q_{max}} \tag{12}$$

Where $\alpha(t)$ represents the reaction degree of slag, $Q(t)$ is the heat release at time t and Q_{max} is the total heat release.

The total heat release was obtained based on the result of reaction degree calculated by selective dissolution at 3d, which is stable. The results of reaction degree and phase transformation is shown in Fig. 10. In order to clearly show the hydrates, the unreacted slag was not shown because of the relatively large amount. At initial hydration process, gypsum and brucite precipitated as observed in XRD (Fig. S2), which also consistent with the results of pore solution. This kind phenomenon inhibits the dissolution of slag. However, the

concentration of Mg^{2+} is not so high and brucite gradually dissolved, this maybe the reason that brucite cannot be detected at 3d. Although the initial hydration was inhibited, large amount of AFt remain for quite a long time because of high concentration of SO_4^{2-} in the pore solution, the formation of AFt increases the solid volume by 164.2%[67]. Therefore, the strength of MS still higher than that of control group.

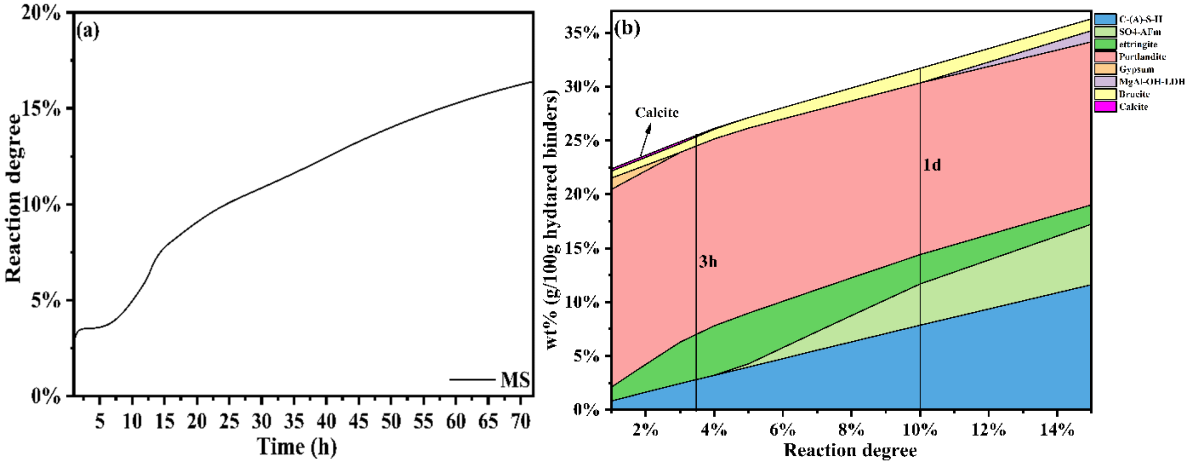

Fig. 10 (a) reaction degree of slag at early age and (b)phase transformation of MS at initial stage

3.5.4.SEM-EDS

Fig. 11 presents the SEM images of the MS paste at 1h and 9h. A large amount of plate-shaped and little needle-like shaped hydrates is observed, which demonstrates the added MS accelerate the dissolution and hydration of slag. In Fig. 11(b), an extent amount of brucite, which has a plate-like shaped similar as $Ca(OH)_2$[68] has been observed. This indicates in MS, the initial hydration kinetics were limited and resulted in the precipitation of brucite, which is consistent with the result of XRD and thermodynamic modelling.

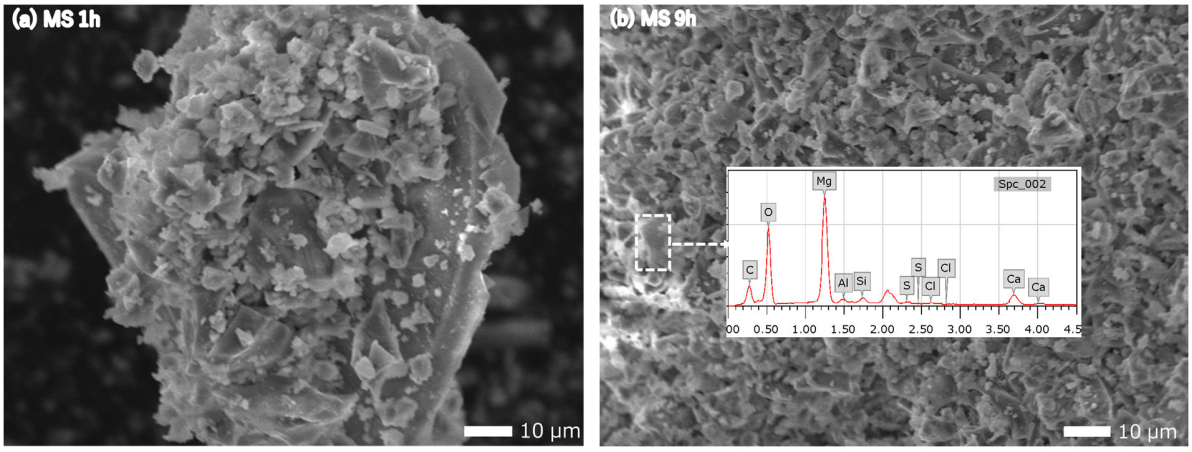

Fig. 11. SEM image of (a) the MS paste at 1h and (b) the MS paste at 9h.

4. Conclusions

In this study, the effects of cations in sulfate on $Ca(OH)_2$ activated GGBFS were mainly investigated by XRD, Isothermal calorimetry, TGA and thermodynamic modeling. The main conclusions are:

1. Although all of the nitrite, chloride and sulfate activators could improve the strength of slag at early age, it seems the type of nitrite and chloride has little impact on the development of slag hydration.
2. Sulfate activators with different cations can promote the compressive strength and hydration degree of $Ca(OH)_2$ activated blast furnace slag at early age as the order: K_2SO_4> Na_2SO_4 > $MgSO_4$, but their strength were comparable to strength of the mortar without activators at 28d.
3. As one of the main hydration products, the type of AFm like phase is quietly dependent on the anion of activators.
4. K_2SO_4 and Na_2SO_4 accelerate the hydration kinetics of pastes evidently because of hydrates like AFm and AFt produced. The hydration kinetics of $MgSO_4$ was limited due to the precipitation of gypsum and brucite at initial stage, which may relate to the change of pH value.
5. The development of compressive strength at early age may relate to the pH change at initial stage. The mechanism of pH change in K_2SO_4 and Na_2SO_4 is almost same, a rise on pH can be achieved due to synergistic reactions between sulfate and $Ca(OH)_2$, while the low pH of $MgSO_4$ is mainly due to the low solubility of brucite and precipitation of gypsum. The critical concentration of calcium ions is 20mM and critical pH value is around 13.1 for promoting the slag hydration in this study.
6. Compared with K_2SO_4 and Na_2SO_4, although the hydration process in $MgSO_4$ is lower, a large amount of AFt remain due to the high concentration of SO_4^{2-}, which can still promote the strength development at early age.

Acknowledgement

This work was supported by JSPS KAKENHI Grant Number 21K04349 and the Steel Foundation for Environmental Protection Technology.

Reference

[1] J. Bijen, Benefits of slag and fly ash, Constr. Build. Mater. 10 (1996). https://doi.org/10.1016/0950-0618(95)00014-3.

[2] K.C. Reddy, K.V.L. Subramaniam, Blast Furnace Slag Hydration in an Alkaline Medium: Influence of Sodium Content and Sodium Hydroxide Molarity, J. Mater. Civ. Eng. 32 (2020) 04020371. https://doi.org/10.1061/(asce)mt.1943-5533.0003455.

[3] X. Dai, S. Aydın, M.Y. Yardımcı, K. Lesage, G. De Schutter, Effect of ca(Oh)2 addition on the engineering properties of sodium sulfate activated slag, Materials (Basel). 14 (2021). https://doi.org/10.3390/ma14154266.

[4] Y. Jeong, J.E. Oh, Y. Jun, J. Park, J.H. Ha, S.G. Sohn, Influence of four additional activators on hydrated-lime [Ca(OH)2] activated ground granulated blast-furnace slag, Cem. Concr. Compos. 65 (2016) 1–10. https://doi.org/10.1016/j.cemconcomp.2015.10.007.

[5] R. Kondo, C.T. Song, S. Goto, M. Daimon, Latent Hydraulic Property of Granulated Blast Furnace Slag By Various Activators., Tetsu-To-Hagane/Journal Iron Steel Inst. Japan. 65 (1979) 1825–1829. https://doi.org/10.2355/tetsutohagane1955.65.13_1825.

[6] M. Shariati, A. Shariati, N.T. Trung, P. Shoaei, F. Ameri, N. Bahrami, S.N. Zamanabadi, Alkali-activated slag (AAS) paste: Correlation between durability and microstructural characteristics, Constr. Build. Mater. 267 (2021). https://doi.org/10.1016/j.conbuildmat.2020.120886.

[7] C. Shi, J. Qian, High performance cementing materials from industrial slags - A review, Resour. Conserv. Recycl. 29 (2000). https://doi.org/10.1016/S0921-3449(99)00060-9.

[8] E. Gartner, Industrially interesting approaches to “low-CO2” cements, Cem. Concr. Res. 34 (2004). https://doi.org/10.1016/j.cemconres.2004.01.021.

[9] H. Beushausen, M. Alexander, Y. Ballim, Early-age properties, strength development and heat of hydration of concrete containing various South African slags at different replacement ratios, Constr. Build. Mater. 29 (2012). https://doi.org/10.1016/j.conbuildmat.2011.06.018.

[10] S.D. Wang, X.C. Pu, K.L. Scrivener, P.L. Pratt, Alkali-activated slag cement and concrete: A review of properties and problems, Adv. Cem. Res. 7 (1995). https://doi.org/10.1680/adcr.1995.7.27.93.

[11] X. Wu, W. Jiang, D.M. Roy, Early activation and properties of slag cement, Cem. Concr. Res. 20 (1990). https://doi.org/10.1016/0008-8846(90)90060-B.

583 [12] R.J. Thomas, B.S. Gebregziabiher, A. Giffin, S. Peethamparan, Micromechanical
584 properties of alkali-activated slag cement binders, Cem. Concr. Compos. 90 (2018).
585 https://doi.org/10.1016/j.cemconcomp.2018.04.003.

586 [13] H.A. Nguyen, T.P. Chang, A. Thymotie, Enhancement of early engineering
587 characteristics of modified slag cement paste with alkali silicate and sulfate, Constr.
588 Build. Mater. 230 (2020). https://doi.org/10.1016/j.conbuildmat.2019.117013.

589 [14] G. Xu, Q. Tian, J. Miao, J. Liu, Early-age hydration and mechanical properties of high
590 volume slag and fly ash concrete at different curing temperatures, Constr. Build. Mater.
591 149 (2017) 367–377. https://doi.org/10.1016/j.conbuildmat.2017.05.080.

592 [15] S.D. Wang, K.L. Scrivener, P.L. Pratt, Factors affecting the strength of alkali-activated
593 slag, Cem. Concr. Res. 24 (1994). https://doi.org/10.1016/0008-8846(94)90026-4.

594 [16] A.M. Rashad, Y. Bai, P.A.M. Basheer, N.B. Milestone, N.C. Collier, Hydration and
595 properties of sodium sulfate activated slag, Cem. Concr. Compos. 37 (2013).
596 https://doi.org/10.1016/j.cemconcomp.2012.12.010.

597 [17] B.S. Gebregziabiher, R.J. Thomas, S. Peethamparan, Temperature and activator effect
598 on early-age reaction kinetics of alkali-activated slag binders, Constr. Build. Mater.
599 113 (2016). https://doi.org/10.1016/j.conbuildmat.2016.03.098.

600 [18] M. Ben Haha, G. Le Saout, F. Winnefeld, B. Lothenbach, Influence of activator type
601 on hydration kinetics, hydrate assemblage and microstructural development of alkali
602 activated blast-furnace slags, Cem. Concr. Res. 41 (2011).
603 https://doi.org/10.1016/j.cemconres.2010.11.016.

604 [19] A. Fernandez-Jimenez, F. Puertas, Effect of activator mix on the hydration and
605 strength behaviour of alkali-activated slag cements, Adv. Cem. Res. 15 (2003).
606 https://doi.org/10.1680/adcr.15.3.129.36623.

607 [20] S. Song, H.M. Jennings, Pore solution chemistry of alkali-activated ground granulated
608 blast-furnace slag, Cem. Concr. Res. 29 (1999). https://doi.org/10.1016/S0008-
609 8846(98)00212-9.

610 [21] G.C. Edwards, R.L. Angstadt, The effect of some soluble inorganic admixtures on the
611 early hydration of portland cement, J. Appl. Chem. 16 (2007).
612 https://doi.org/10.1002/jctb.5010160508.

613 [22] A.K. Suryavanshi, J.D. Scantlebury, S.B. Lyon, Mechanism of Friedel's salt formation
614 in cements rich in tri-calcium aluminate, Cem. Concr. Res. 26 (1996).
615 https://doi.org/10.1016/S0008-8846(96)85009-5.

616 [23] F. Barberon, V. Baroghel-Bouny, H. Zanni, B. Bresson, J.B. D'Espinose De La
617 Caillerie, L. Malosse, Z. Gan, Interactions between chloride and cement-paste
618 materials, in: Magn. Reson. Imaging, 2005. https://doi.org/10.1016/j.mri.2004.11.021.

[24] M. Collin, D.P. Prentice, R.A. Arnold, K. Ellison, D.A. Simonetti, G.N. Sant, Fly Ash-Ca(OH)2Reactivity in Hypersaline NaCl and CaCl2Brines, ACS Sustain. Chem. Eng. (2021). https://doi.org/10.1021/acssuschemeng.1c01884.

[25] Y. Sun, J.X. Lu, C.S. Poon, Strength degradation of seawater-mixed alite pastes: an explanation from statistical nanoindentation perspective, Cem. Concr. Res. 152 (2022) 106669. https://doi.org/10.1016/j.cemconres.2021.106669.

[26] C. Fu, H. Ye, K. Zhu, D. Fang, J. Zhou, Alkali cation effects on chloride binding of alkali-activated fly ash and metakaolin geopolymers, Cem. Concr. Compos. 114 (2020) 103721. https://doi.org/10.1016/j.cemconcomp.2020.103721.

[27] R. Myrdal, SINTEF REPORT: Advanced cementing materials - Controlling hydration development - Accelerating admixtures for concrete - State of the art, 2007. www.sintef.no/coin.

[28] K. De Weerdt, A. Colombo, L. Coppola, H. Justnes, M.R. Geiker, Impact of the associated cation on chloride binding of Portland cement paste, Cem. Concr. Res. 68 (2015). https://doi.org/10.1016/j.cemconres.2014.01.027.

[29] M. Sajid, C. Bai, M. Aamir, Z. You, Z. Yan, X. Lv, Understanding the structure and structural effects on the properties of blast furnace slag (BFS), ISIJ Int. 59 (2019). https://doi.org/10.2355/isijinternational.ISIJINT-2018-453.

[30] J. da S. Andrade Neto, A.G. De la Torre, A.P. Kirchheim, Effects of sulfates on the hydration of Portland cement – A review, Constr. Build. Mater. 279 (2021). https://doi.org/10.1016/j.conbuildmat.2021.122428.

[31] B. Mota, T. Matschei, K. Scrivener, Impact of NaOH and Na2SO4 on the kinetics and microstructural development of white cement hydration, Cem. Concr. Res. 108 (2018). https://doi.org/10.1016/j.cemconres.2018.03.017.

[32] Q. Zhai, K. Kurumisawa, Effect of accelerators on Ca(OH)2 activated ground granulated blast-furnace slag at low curing temperature, Cem. Concr. Compos. 124 (2021) 104272. https://doi.org/10.1016/j.cemconcomp.2021.104272.

[33] J. Fu, A.M. Jones, M.W. Bligh, C. Holt, L.M. Keyte, F. Moghaddam, S.J. Foster, T.D. Waite, Mechanisms of enhancement in early hydration by sodium sulfate in a slag-cement blend – Insights from pore solution chemistry, Cem. Concr. Res. 135 (2020) 106110. https://doi.org/10.1016/j.cemconres.2020.106110.

[34] C. Science, C. Technology, 1. 2. 2. 1, 74 (n.d.) 105–110.

[35] H. Justnes, T.A. Østnor, Designing alternative binders utilizing synergistic reactions, in: Am. Concr. Institute, ACI Spec. Publ., 2015.

[36] N. Doebelin, R. Kleeberg, Profex: A graphical user interface for the Rietveld refinement program BGMN, J. Appl. Crystallogr. 48 (2015). https://doi.org/10.1107/S1600576715014685.

656 [37] A Practical Guide to Microstructural Analysis of Cementitious Materials, 2018.
657 https://doi.org/10.1201/b19074.

658 [38] Y.A. Villagrán-Zaccardi, A. Vollpracht, E. Gruyaert, N. De Belie, Recommendation
659 of RILEM TC 238-SCM: determination of the degree of reaction of siliceous fly ash
660 and slag in hydrated cement paste by the selective dissolution method, Mater. Struct.
661 Constr. 51 (2018). https://doi.org/10.1617/s11527-017-1134-3.

662 [39] Z. Bian, G. Jin, T. Ji, Effect of combined activator of Ca(OH)2 and Na2CO3 on
663 workability and compressive strength of alkali-activated ferronickel slag system, Cem.
664 Concr. Compos. 123 (2021) 104179.
665 https://doi.org/10.1016/j.cemconcomp.2021.104179.

666 [40] S.A. Bernal, M.C.G. Juenger, X. Ke, W. Matthes, B. Lothenbach, N. De Belie, J.L.
667 Provis, Characterization of supplementary cementitious materials by thermal analysis,
668 Mater. Struct. Constr. 50 (2017). https://doi.org/10.1617/s11527-016-0909-2.

669 [41] B. Lothenbach, F. Winnefeld, Thermodynamic modelling of the hydration of Portland
670 cement, Cem. Concr. Res. 36 (2006).
671 https://doi.org/10.1016/j.cemconres.2005.03.001.

672 [42] F.J. Tang, E.M. Gartner, Influence of sulphate source on Portland cement hydration,
673 Adv. Cem. Res. 1 (1988). https://doi.org/10.1680/adcr.1988.1.2.67.

674 [43] R. Trauchessec, J.M. Mechling, A. Lecomte, A. Roux, B. Le Rolland, Hydration of
675 ordinary Portland cement and calcium sulfoaluminate cement blends, Cem. Concr.
676 Compos. 56 (2015). https://doi.org/10.1016/j.cemconcomp.2014.11.005.

677 [44] Y. Ma, J. Qian, Influence of alkali sulfates in clinker on the hydration and hardening
678 of Portland cement, Constr. Build. Mater. 180 (2018).
679 https://doi.org/10.1016/j.conbuildmat.2018.05.196.

680 [45] Y. Briki, F. Avet, M. Zajac, P. Bowen, M. Ben Haha, K. Scrivener, Understanding of
681 the factors slowing down metakaolin reaction in limestone calcined clay cement (LC3)
682 at late ages, Cem. Concr. Res. 146 (2021).
683 https://doi.org/10.1016/j.cemconres.2021.106477.

684 [46] J. Fu, M.W. Bligh, I. Shikhov, A.M. Jones, C. Holt, L.M. Keyte, F. Moghaddam, C.H.
685 Arns, S.J. Foster, T.D. Waite, A microstructural investigation of a Na2SO4 activated
686 cement-slag blend, Cem. Concr. Res. 150 (2021).
687 https://doi.org/10.1016/j.cemconres.2021.106609.

688 [47] O.R. Ogirigbo, L. Black, Influence of slag composition and temperature on the
689 hydration and microstructure of slag blended cements, Constr. Build. Mater. 126
690 (2016). https://doi.org/10.1016/j.conbuildmat.2016.09.057.

691 [48] P. Li, J. Tang, X. Chen, Y. Bai, Q. Li, Effect of temperature and pH on early hydration
692 rate and apparent activation energy of alkali-activated slag, Adv. Mater. Sci. Eng. 2019
693 (2019). https://doi.org/10.1155/2019/3531543.

694 [49] T. Bakharev, J.G. Sanjayan, Y.B. Cheng, Effect of elevated temperature curing on
695 properties of alkali-activated slag concrete, Cem. Concr. Res. 29 (1999).
696 https://doi.org/10.1016/S0008-8846(99)00143-X.

697 [50] Y. Briki, M. Zajac, M. Ben Haha, K. Scrivener, Factors affecting the reactivity of slag
698 at early and late ages, Cem. Concr. Res. 150 (2021) 106604.
699 https://doi.org/10.1016/j.cemconres.2021.106604.

700 [51] R. Kondo, M. Daimon, E. Sakai, H. Ushiyama, Influence of inorganic salts on the
701 hydration of tricalcium silicate, J. Biochem. Toxicol. 27 (1977) 191–197.
702 https://doi.org/10.1002/jbt.2570270128.

703 [52] C. Shi, R.L. Day, Chemical activation of blended cements made with lime and natural
704 pozzolans, Cem. Concr. Res. 23 (1993). https://doi.org/10.1016/0008-8846(93)90076-
705 L.

706 [53] C. Shi, D. Roy, P. Krivenko, Alkali-Activated Cements and Concretes, 2003.
707 https://doi.org/10.1201/9781482266900.

708 [54] K.H. Yang, A.R. Cho, J.K. Song, S.H. Nam, Hydration products and strength
709 development of calcium hydroxide-based alkali-activated slag mortars, Constr. Build.
710 Mater. 29 (2012). https://doi.org/10.1016/j.conbuildmat.2011.10.063.

711 [55] T. Bakharev, J.G. Sanjayan, Y.B. Cheng, Sulfate attack on alkali-activated slag
712 concrete, Cem. Concr. Res. 32 (2002). https://doi.org/10.1016/S0008-8846(01)00659-
713 7.

714 [56] L. Nedyalkova, B. Lothenbach, G. Geng, U. Mäder, J. Tits, Uptake of iodide by
715 calcium aluminate phases (AFm phases), Appl. Geochemistry. 116 (2020).
716 https://doi.org/10.1016/j.apgeochem.2020.104559.

717 [57] M. Balonis, M. Mędala, F.P. Glasser, Influence of calcium nitrate and nitrite on the
718 constitution of AFm and AFt cement hydrates, Adv. Cem. Res. 23 (2011) 129–143.
719 https://doi.org/10.1680/adcr.10.00002.

720 [58] M. Balonis, F.P. Glasser, Calcium nitrite corrosion inhibitor in portland cement:
721 Influence of nitrite on chloride binding and mineralogy, J. Am. Ceram. Soc. 94 (2011)
722 2230–2241. https://doi.org/10.1111/j.1551-2916.2010.04362.x.

723 [59] E. Bernard, B. Lothenbach, F. Le Goff, I. Pochard, A. Dauzères, Effect of magnesium
724 on calcium silicate hydrate (C-S-H), Cem. Concr. Res. 97 (2017).
725 https://doi.org/10.1016/j.cemconres.2017.03.012.

726 [60] L. Alarcon-Ruiz, G. Platret, E. Massieu, A. Ehrlacher, The use of thermal analysis in
727 assessing the effect of temperature on a cement paste, Cem. Concr. Res. 35 (2005).
728 https://doi.org/10.1016/j.cemconres.2004.06.015.

729 [61] B. Xu, Y. Yi, Use of ladle furnace slag containing heavy metals as a binding material
730 in civil engineering, Sci. Total Environ. 705 (2020).
731 https://doi.org/10.1016/j.scitotenv.2019.135854.

[62] N. Ukrainczyk, M. Ukrainczyk, J. Sipusic, T. Matusinovic, XRD and TGA Investigation of Hardened Cement Paste, 11. Conf. Mater. Process. Frict. Wear MATRIB'06, Vela Luka. (2006).

[63] P.T. Durdziński, M. Ben Haha, M. Zajac, K.L. Scrivener, Phase assemblage of composite cements, Cem. Concr. Res. 99 (2017). https://doi.org/10.1016/j.cemconres.2017.05.009.

[64] Y.A. Villagrán-Zaccardi, H. Egüez-Alava, K. De Buysser, E. Gruyaert, N. De Belie, Calibrated quantitative thermogravimetric analysis for the determination of portlandite and calcite content in hydrated cementitious systems, Mater. Struct. Constr. 50 (2017). https://doi.org/10.1617/s11527-017-1046-2.

[65] P. Suraneni, M. Palacios, R.J. Flatt, New insights into the hydration of slag in alkaline media using a micro-reactor approach, Cem. Concr. Res. 79 (2016). https://doi.org/10.1016/j.cemconres.2015.09.015.

[66] Y. Cai, D. Xuan, P. Hou, J. Shi, C.S. Poon, Effect of seawater as mixing water on the hydration behaviour of tricalcium aluminate, Cem. Concr. Res. 149 (2021). https://doi.org/10.1016/j.cemconres.2021.106565.

[67] C. Shi, R.L. Day, Pozzolanic reaction in the presence of chemical activators, Cem. Concr. Res. 30 (2000) 51–58. https://doi.org/10.1016/s0008-8846(99)00205-7.

[68] N. Ranjbar, C. Kuenzel, J. Spangenberg, M. Mehrali, Hardening evolution of geopolymers from setting to equilibrium: A review, Cem. Concr. Compos. 114 (2020). https://doi.org/10.1016/j.cemconcomp.2020.103729.